REVIEWS OF ATMOSPHERIC SCIENCE TOPICS, VOL. 12, X, DOI:10.1029/,

The History behind the Discovery of the Earth's Atmospheric Composition

Cassandra Gaston

Scripps Institute of Oceanography, University of California, San Diego, CA, USA

Aneesh C. Subramanian

Scripps Institute of Oceanography, University of California, San Diego, CA, USA

Melanie Zauscher

Department of Mechanical and Aerospace Engineering, University of California, San Diego, CA, USA

Abstract. The discovery of the five main constituents of the atmosphere along with their corresponding abundance spans more than 2000 years. A historical overview of the most significant of these findings is presented with attention given to the discoveries and measurements of the abundance of each of these constituents between 1450 through 1910, when almost all the constituents of air were discovered and tabulated. The initial measurements of the constituents of air, with the exception of argon, were later improved and summarized in the early 1800s by John Dalton. These types of measurements are key to understanding how the natural abundances of atmospheric gases are currently changing due to anthropogenic emissions including air pollution and greenhouse gases.

1. Introduction

The ancient Greeks were the first to recognize air as being a key element of the earth. Although Aristotle theorized that water was a component of air in the form of clouds and rain [*Aristotle* [350 B. C.], *Humphreys* [1927]], it was only around 1450 that Nicolas de Cusa became the first to quantitatively measure atmospheric water vapor with a hygrometer providing more concrete evidence of a multi-component atmosphere [*Pagel*, 1982]. The philosophies regarding the nature of air changed dramatically around the 1770s when scientists were beginning to learn how to capture and study gases. Due to the discovery of oxygen, nitrogen, and carbon dioxide by 1775, the atmosphere was believed to contain four components. A five component view of the atmosphere, as shown in Table 1, became dominant once Argon was discovered in 1894 [*Ramsay*, 1915].

The discoveries of the atmospheric composition consisted of separating and identifying gases in air by their basic chemical properties. The abundances were all calculated by measuring a simple mass or volume displacement during a chemical reaction. The discovery of the five main atmospheric components and their abundance is the subject of the remainder of this paper; the discussion is chronological and broken into five sections.

2. Discovery of the Major Atmospheric Constituents

2.1. Water Vapor

Although water vapor was the first component of air to be identified due to its presence in rain and other perceivable forms, it was not officially discovered or measured until 1450. Nicholas de Cusa was the first to do this using a hygrometer, an instrument used even today to measure water vapor content of air. Cusa's hygrometer used wool to absorb

moisture from the air and the corresponding change in the weight of the wool was used to calculate atmospheric humidity. His measurements, however, were highly inaccurate [*Pagel*, 1982].

In 1802, John Dalton [*Truesdon*, 2006] was the first to accurately measure the water vapor in air, as shown in Table 1. Dalton tabulated the values of water vapor pressure for every degree of temperature variation in the atmosphere, showing that the percent of water vapor in atmosphere is variable between 0.44 to 1.44% by weight. A more precise measurement of vapor pressures of water vapor at different temperatures of air was later published by Ramsay and Young [*Ramsay and Young*, 1892], by measuring the water vapor pressure and correcting for experimental errors using the ideal gas law equations.

2.2. Carbon dioxide

Johann Baptist van Helmont discovered carbon dioxide when he burned charcoal in a closed vessel and observed that this gas evolved from the reaction [*Pagel*, 1982]. It was observed that it did not support flame or life. Joseph Black, in 1751, was the first to deduce that carbon dioxide was a constituent of air by burning magnesia alba (hydrated magnesium carbonate) and observing the weight difference in the burnt mixture and surrounding air [*Black*, 1756].

In 1800, Alexander Von Humboldt was one of the first to quantify atmospheric carbon dioxide by placing plants in a closed photosynthesis chamber and measuring the change in volume associated with carbon dioxide uptake by plants. From this, he measured carbon dioxide to be 1% by weight of air [*Humboldt*, 1858], which is over 30 times greater than the known concentration listed in Table 1. Theodore de Saussure made the first detailed measurements of atmospheric carbon dioxide in 1804 by carefully weighing the amount of

organic matter and oxygen the plants produced [*Rabinowitch* [1971], *Black* [1756]]. The mean atmospheric value he found was 0.04% by volume.

2.3. Oxygen

Oxygen was discovered independently by both Carl Scheele in 1772 and Joseph Priestley in 1774; however, Priestley was the first to publish his findings [*Lenton*, 2003]. Priestley discovered oxygen when he heated mercury oxide and observed that the gas released caused a flame enlargement [*Toulmin*, 1957]. His discovery was later expanded upon by Antoine Lavoisier who realized that this new gas could support combustion. Since air also supports combustion, he theorized that this new gas was a component of the atmosphere. In 1779, Lavoisier decided to test his theory using an inverted bottle that trapped a fixed amount of air. A flask, in contact with the bottle, contained mercury and reacted with the oxygen in the bottle creating a volume displacement. The change in volume led Lavoisier to conclude that this new gas constituted about one-fifth of the volume of air [*Harley* [1947], *Toulmin* [1957]].

A more accurate measurement of oxygen content in air was obtained by Henry Cavendish in 1783. Using the same type of experiment as Lavoisier where a fixed amount of air was used for a combustion reaction, Cavendish repeatedly burned phosphorus with the same air until it would no longer combust. He calculated the percent volume of oxygen in air to be 20.83% [*Dalton* [1805], *Cavendish et al.* [1879]].

2.4. Nitrogen

In 1772, Daniel Rutherford was the first to publish experiments identifying nitrogen [*Ramsay*, 1915]. In confined air, Rutherford removed the oxygen by burning phosphorus

[*Humphreys*, 1927]. He then removed carbon dioxide from the remaining gas sample with potash. The remaining gas was foul smelling and poisonous to life, so Rutherford named it "mephitic air" after the Latin mephitis, for noxious stench.

Cavendish was the first person to measure the abundance of nitrogen in air in 1783 [*Weeks*, 1934]. After removing nitrogen and oxygen from air by reacting it with nitric oxide and potash, he isolated atmospheric nitrogen [*Ramsay*, 1915]. Cavendish determined the concentration of atmospheric nitrogen to be 79.16% [*Ramsay*, 1915].

2.5. Argon

During his experiments in the 1780s, Cavendish used a frictional apparatus that supplied electricity to isolated air and oxygen reducing atmospheric nitrogen to nitrous acid, which he removed with potash [*Giunta*, 1998]. Despite the fact that he kept this experiment working for weeks, there was still a 1/120th part of the total gaseous sample unabsorbed [*Cavendish*, 1785]. Although Cavendish suspected this was due to the presence of a separate inert gas, he was not able to prove his conjecture [*Cederblom*, 1904].

Argon was officially identified and quantified a century later by Rayleigh and Ramsay [*Rayleigh*, 1892]. Having a reliable source of electricity, they repeated Cavendish's experiment and were finally able to isolate enough of this gas to study it [*Rayleigh*, 1895]. For every liter of the gas they isolated, they had to use 100 liters of nitrogen. From this, they estimated the unidentified gas makes up 1% of air, which is in close agreement with the accepted value listed in Table 1 [*Rayleigh*, 1895]. After performing identification tests, they realized they had isolated a new element when the ratio of heat capacities indicated it was a monatomic gas [*Ramsay*, 1904]. Rayleigh and Ramsay named this monatomic gas argon, Greek for inert, since it did not react with anything.

3. Conclusions

The discoveries of water vapor, carbon dioxide, oxygen, nitrogen, and argon in the atmosphere, performed by de Cusa, Black, Lavoisier, Rutherford, and Ramsay and Rayleigh respectively, led to quantifying their abundance. These measurements consisted of calculating the change in a volume of air consumed from a combustion reaction, as was the case for both oxygen and nitrogen, or consumed by biological reactions, as was the case for measuring carbon dioxide. Subsequent abundances were calculated by measuring the amount of gas that was chemically and energetically unreactive as was the case with argon, and weighing the amount of moisture that could be collected for a given amount of air. Calculating the concentration of water vapor and carbon dioxide have been particularly difficult tasks due to the variability of water vapor and the techniques used to isolate carbon dioxide. These initial calculations, however, were improved by John Dalton who measured each gas with the exception of argon. In 1805, Dalton improved the experiments of Lavoisier, Cavendish, and von Humboldt to obtain these abundances using a mass displacement instead of a volume displacement [*Dalton*, 1805].

The significance of these abundance measurements has become increasingly apparent as humans have been changing the composition of the earth's atmosphere through activities such as fossil fuel combustion. If these changes in abundance had not been detected, the need to curb emissions of greenhouse gases, such as carbon dioxide would not be known. Although these changes in abundance are small, they have the ability to have long-lasting consequences for the earth's climate.

References

Aristotle (350 B. C.), Meteorology.

Black, J. (1756), Experiments upon magnesia alba, quick lime and some other alkaline substances.

Cavendish, H. (1785), Experiments on air, *Philosophical Transactions*, *75*, 372.

Cavendish, H., J. C. Maxwell, J. Larmor, and T. Thorpe (1879), *The Scientific Papers of the Honourable Henry Cavendish*, vol. I, Cambridge University Press.

Cederblom, J. E. (1904), Presentation speech for the nobel prize in chemistry.

Curry, J. A., and P. J. Webster (1999), *Thermodynamics of the Atmosphere and Oceans*, Academic Press.

Dalton, J. (1805), Experimental enquiry into the proportion of the several gases or elastic fluids, constituting the atmosphere, *Memoirs of the Literary and Philosophical Society of Manchester 1*, pp. 244 – 258.

Giunta, C. J. (1998), Using history to teach science: the case of argon, *J. J. Chem. Educ.*, *75*, 1322–1325.

Harley, H. (1947), Antoine laurent lavoisier, *Proceedings of the Royal Society of London, Series A, Mathematical and Physical Sciences*, pp. 427–456.

Humboldt (1858), *COSMOS: A Sketch of the Physical Description of the Universe*, vol. 1, Harper & Brothers.

Humphreys, W. (1927), The atmosphere: origin and composition, *The Scientific Monthly*, *24(3)*, 214–219.

Lenton, T. M. (2003), *Evolution of Planet Earth: The Impact of the Physical Environment.*, chap. The coupled evolution of life and atmospheric oxygen, Academic Press.

Pagel, W. (1982), *Joan Baptista van Helmont: Reformer of Science and Medicine*, Cambridge Univ. Pr., West Nyack, New York, U. S. A.

Rabinowitch, E. (1971), An unfolding discovery, *Proceedings of the National Academy of Sciences of the United States of America*, *68*(11), 2875–2876.

Ramsay, W. (1904), The rare gases of the atmosphere.

Ramsay, W. (1915), *The gases of the atmosphere*, 4th ed., MacMillan and Co., London.

Ramsay, W., and S. Young (1892), On some of the properties of water and steam, *Philosophical Transactions of the Royal Society of London. A*, *183*, 107–130.

Rayleigh, L. (1892), Density of nitrogen, *Nature*, *46*, 512.

Rayleigh, L. (1895), Argon, *Royal Institution Proceedings*, *14*, 524–538.

Toulmin, S. E. (1957), Crucial experiments: Priestley and lavoisier, *Journal of the History of Ideas*.

Truesdon, J. (2006), Physical science ii.

Weeks, M. (1934), Daniel rutherford and the discovery of nitrogen, *J. Chem. Educ.*, *11*, 101–110.

Table 1. Main Gaseous Constituents of Air (Modified from [*Curry and Webster*, 1999])

Constituents	Abundance [Cavendish, 1783](% Volume)	[Dalton, 1805] (% mass)	Accepted Abundance (% Volume)	Accepted Abundance (% mass)
Nitrogen	79.16	75.55	78.08	75.51
Oxygen	20.84	23.32	20.95	23.14
Argon	-	-	0.93	1.28
Carbon Dioxide	-	0.10	0.03	0.05
Water Vapor	-	0.44 - 1.03	0 - 4	-

REVIEWS OF ATMOSPHERIC SCIENCE TOPICS, VOL. 12, X, DOI:10.1029/,

Advances in understanding atmospheric composition: Changes in CO_2 and water vapor content

Cassandra Gaston

Scripps Institution of Oceanography, University of California, San Diego,

CA, USA

Aneesh C. Subramanian

Scripps Institution of Oceanography, University of California, San Diego,

CA, USA

Melanie Zauscher

Department of Mechanical and Aerospace Engineering, University of

California, San Diego, CA, USA

Abstract. The chemical composition of the atmosphere is changing due to human activities. The magnitude and spatial scope of these changes have been debatable primarily due to uncertainties in terrestrial and oceanic carbon sinks as well as the extent of the increase of water vapor in the atmosphere. Recent advances in 2005 by Bender *et al.* and Soden *et al.* have provided evidence that carbon dioxide sinks are quickly reaching saturation while water vapor content has increased substantially in the upper troposphere. Both of these findings have profound effects for predicting future temperature changes due to climate change.

1. Introduction

The increase in carbon dioxide (CO_2) due to fossil fuel combustion was first recognized by G. S. Callendar in 1938 and later substantiated by C. Keeling in the 1950s [*Callendar* [1938], *Ramanathan* [1988]]. However, not all of the anthropogenic CO_2 has ended up in the atmosphere because terrestrial biomass and oceans act as sinks for CO_2. Quantifying and understanding the controls in these sinks is important for predicting how climate will change. In 1896, S. Arrhenius was the first to recognize a positive feedback between CO_2, temperature, and water vapor [*Held and Soden*, 2000]. The positive feedback between temperature and water vapor speculated by Arrhenius has been validated for the lower troposphere using radiosonde data, which shows that the Northern Hemisphere has experienced an increase in water vapor due to an increase in temperature [*Ross and Elliot*, 2001]. Changes in the upper troposphere contribute more to the Earth's radiation budget; however, these changes have been difficult to measure due to their small magnitude.

The focus of this paper is to highlight two major advances regarding our understanding of the changing atmospheric composition. The first section describes the sinks of CO_2 quantified by Bender *et al.* [2005]. The next section addresses the increases in water vapor measured in the upper troposphere by Soden *et al.* [2005].

2. Measuring Changes in CO_2 Sinks: advances made by Bender *et al.*

2.1. O_2/N_2 measurements for constraining carbon sinks

Beginning with R. Keeling(1992), the ratio of oxygen (O_2) to nitrogen (N_2) concentrations has been useful for quantifying CO_2 sinks [*Battle et al.* [2000], *Keeling and Shertz* [1992], *Keeling et al.* [1996]]. This ratio is compared to a reference gas and is expressed

as:

$$\delta(O_2/N_2) = \left(\left(\frac{\delta(O_2/N_2)}{\delta(O_2/N_2)_{ref}} \right) - 1 \right) * 10^6 \quad (1)$$

in per meg units , where a change of 4.8 per meg corresponds to a change of 1 ppm in the O2 concentration [*Keeling and Shertz* [1992], *Bender et al.* [1998]]. The decreasing $\delta(O_2/N_2)$ trends are primarily due to combustion of fossil fuels that consumes oxygen, while nitrogen is assumed to be constant since it is inert [*Battle et al.* [2000], *Keeling et al.* [1996]].

2.2. Quantifying the sequestration of CO_2 by the oceans and land

Between 1994-2003, Bender *et al.* [2005] quantified the sinks of CO_2 with $\delta(O_2/N_2)$ and the concentration of CO_2. From atmospheric samples collected in the six sites shown in Figure 1, they calculated $\delta(O_2/N_2)$ by measuring the isotopes of O_2 and N_2 with a mass spectrometer and the concentration of CO_2 with infrared absorption. Figure 2 shows the seasonal, latitudinal and long-term trends of both CO_2 and $\delta(O_2/N_2)$. Having this temporal data and knowing the anthropogenic source of CO_2 through the rate of fossil fuel consumption and cement manufacturing, Bender *et al.* [2005] computed the ocean and land sequestration rates with Model 1. The calculated carbon sequestration rates, as seen in Figure 3, exhibit strong interannual variations. From 1996-2001, land sinks are highly variable, supporting previous observations that the land biomass is responsible for the most variability in CO_2 uptake [*Bender et al.*, 2005]. The authors attributed the large amplitude in the land sink between 1997-1998 to El Niño. Between 1994-2003, about 50% of the anthropogenic emissions were partitioned between the oceans and land as 1.7 ± 0.5 and 1.0 ± 0.6 Gt C/yr respectively [*Bender et al.*, 2005].

2.3. Significance

The study by Bender *et al.* [2005] provides evidence that the sequestration rates of CO_2 from land and ocean vary significantly in time. Figure 3 provides evidence that both the oceans and land are sources of CO_2 during certain periods of time. Battle *et al.* [2005] calculated that between 1977-1990 the land biosphere acted as neither a sink nor a source of CO2 [*Battle et al.*, 1996]. However, in the early 1990s R. Keeling *et al.* [1996] calculated the land acted as a sink for 2.0 ± 0.9 Gt C/yr. The results from Bender *et al.* [2005] show the average rate of CO_2 sequestration from land decreased during 1994-2003. Both R. Keeling *et al.* [1996] and Bender *et al.* [2005] estimated the same annual average ocean sink, so it appears the ocean sink has been steady since 1991. Hence, it is important to understand all the environmental and climatological switches that turn the land biomass from a source to a sink of carbon since the land sink correlates fairly well with the variability of total CO_2 sequestration. It remains unknown how long the oceans and, especially, the land will be able to sequester such a significant amount of anthropogenic emissions.

3. Increases in Upper Tropospheric Water Vapor: Advances by Soden *et al.*

3.1. Clausius-Clayperon and relative humidity

One assumption that climate scientists and climate models make is that atmospheric circulation patterns will maintain a constant relative humidity (H) throughout the temperature changes associated with climate change. As the temperature increases due to greenhouse forcing, the saturation vapor pressure (e_s) increases in accordance with the Clausius-Clapeyron equation. In agreement with the relative humidity equation, $H = e/e_s(T)$, as the saturation vapor pressure is rising, the vapor pressure (e), and thus water vapor con-

tent, must also rise in order to maintain constant relative humidity [*Held and Soden*, 2000]. This assumption of constant relative humidity has been shown to be accurate for the lower troposphere [*Ross and Elliot*, 2001]; however, the validity of this assumption for the upper troposphere was debated until the work of Soden *et al.* (2005) was published.

3.2. Observational evidence for increasing water vapor

Soden *et al.* [2005] have proven conclusively that water vapor content in the upper troposphere is increasing. Two sets of satellite data that spans 22 years (1982-2004) were used to confirm this result. The High Resolution Infrared Radiometer Sounder (HIRS) uses a 6.3μm water vapor absorption band to measure water vapor over the upper troposphere. Using clear-sky conditions to minimize the influence of clouds, Soden *et al.*[2005] analyzed anomalies created by this satellite, which are functions of both changes in temperature and water vapor. The Microwave Sounding Unit (MSU) measures temperature in the upper troposphere. The difference between these two signals provides observational data for the water vapor increase in the upper troposphere. The authors compared the data to two GCM simulations: relative humidity was kept constant in the first scenario and relative humidity was allowed to change in the second scenario. As seen in Figure 4, the observational data from the two satellites and the modeled results that maintain constant relative humidity correlate very well [*Soden et al.*, 2005].

3.3. Significance to the field

Soden's study disproves earlier theories that water vapor would decrease in the upper troposphere in a warming climate. For instance, R. Lindzen speculated that deep cumulus convection would increase creating towers of rapidly rising moist air that would precipitate

out almost all of their water content creating dry air. This dry air would then subside creating a drier troposphere above 5km ([*Lindzen*, 1990], see figure 5). Furthermore, the modeled results that keep relative humidity constant throughout the troposphere and, therefore, produce an increase in the water vapor content of the upper troposphere match the satellite observed data almost perfectly [*Soden et al.*, 2005]. This discovery provides merit for using the assumption that relative humidity is conserved and validates the use of climate models for predicting future climate changes [*Cess*, 2005]. The increased water vapor content of the upper troposphere also has an overall impact on the climate. As water vapor increases, the temperature increases in response. Since both water vapor and atmospheric CO_2 are increasing, the combined effect on the Earth's temperature creates an even larger increase.

4. Conclusions

The advance made by Bender *et al.* [2005] provides compelling evidence that carbon sinks are not permanent and will result in larger atmospheric increases in CO_2 once they are exhausted. This conclusion complements the results obtained by Soden *et al.* [2005], which show that water vapor has increased significantly in the upper troposphere. The increase in concentration of these two gases has profound impacts for the sensitivity of the Earth's climate to fossil fuel burning. As less CO_2 is taken up by the ocean and land, more of this greenhouse gas will be available in the atmosphere. This increase of CO_2 will lead to a warmer climate causing the water vapor content of the troposphere to increase. This causes the temperature to increase even further, thus, creating a positive feedback loop between water vapor and temperature. The increase in water vapor as well as the

partitioning of CO_2 between the atmosphere and carbon sinks needs to be refined even further in order for climate models to accurately predict future changes in temperature.

References

Battle, M. L. Bender, P. P. Tans, J. W. C. White, J. T. Ellis, T. Conway, and R. J. Francey (2000), Global carbon sinks and their variability inferred from atmospheric o_2 and $c^{\delta 13}$, *Science*, *287*, 2467–2470.

Battle, M., et al. (1996), Atmospheric gas concentrations over the past century measured in air from firn at the south pole., *Nature*, *383*, 231–235.

Bender, M. L., M. Battle, and R. F. Keeling (1998), The o_2 balance of the atmosphere: a tool for studying the fate of fossil-fuel co_2, *Annu. Rev. Energy Environ.*, *23*, 207–223.

Bender, M. L., D. T. Ho, M. B. Hendricks, R. Mika, M. O. Battle, P. P. Tans, T. J. Conway, B. Sturtevant, and N. Cassar (2005), Atmospheric o_2/n_2 changes, $1993-2002$: Implications for the partitioning of fossil fuel co_2 sequestration, *Global Biogeochemical Cycles*, *19*, 4017.

Callendar, G. S. (1938), The artificial production of carbon dioxide and its influence on temperature., *Q. J. R. Meteorol. Soc.*, *64*, 223–240.

Cess, R. D. (2005), Water vapor feedback in climate models, *Science*, *310*, 795–796.

Held, I. M., and B. J. Soden (2000), Water vapor feedback and global warming, *Annu. Rev. Energy Environ.*, *25*, 441–475.

Keeling, R. F., and S. R. Shertz (1992), Seasonal and interannual variations in atmospheric oxygen and implications for the global carbon-cycle, *Nature*, *358*(6389), 723–727.

Keeling, R. F., S. C. Piper, and M. Heimann (1996), Global and hemispheric co2 sinks deduced from changes in atmospheric o_2 concentration, *Nature*, *381*(6579), 218–221.

Lindzen, R. S. (1990), Some coolness concerning global warming, *Bulletin American Meteorological Society*, *71*(3), 288–299.

Marland, G., T. A. Boden, and R. J. Andres (2003), Global, regional, and national fossil fuel co2 emissions, in *Trends: A Compendium of Data on Global Change*, Oak Ridge Natl. Lab., Oak Ridge, Tenn.

Ramanathan, V. (1988), The greenhouse theory of climate change: a test by an inadvertent global experiment, *Science*, *240*, 293–299.

Ross, R. J., and W. P. Elliot (2001), Radiosonde-based northern hemisphere tropospheric water vapor trends, *Journal of Climate*, *14*, 1602–1622.

Soden, B. J., D. L. Jackson, V. Ramaswamy, M. Schwarzkopf, and X. Huang (2005), The radiative signature of upper tropospheric moistening, *Science*, *310*, 841 – 844.

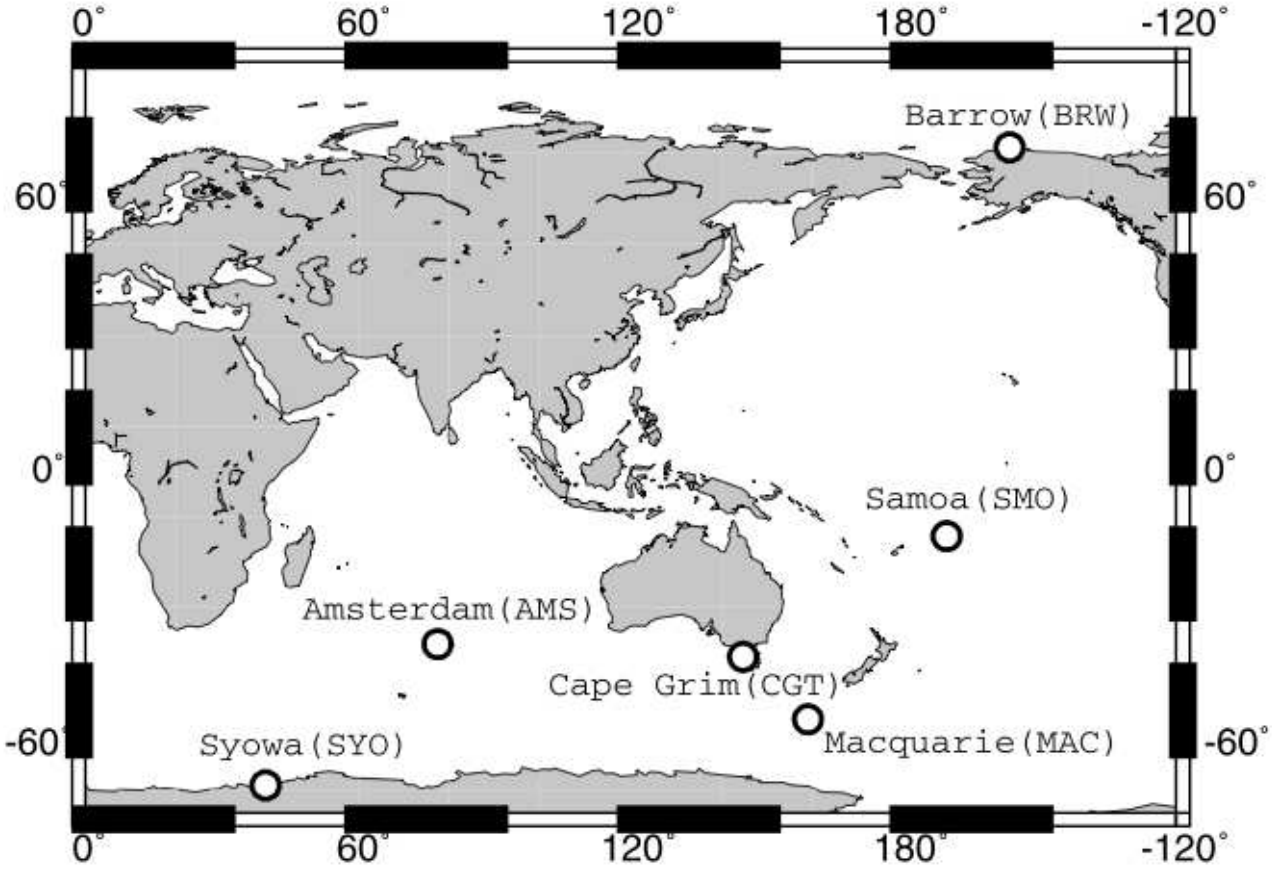

Figure 1. Sampling sites for Bender *et al.* [2005] study. Sites are located in remote areas so that there is no influence from localized pollution plumes. The CO_2 and O_2/N_2 measurements are intended to represent regional, if not global, trends. [*Bender et al.*, 2005]

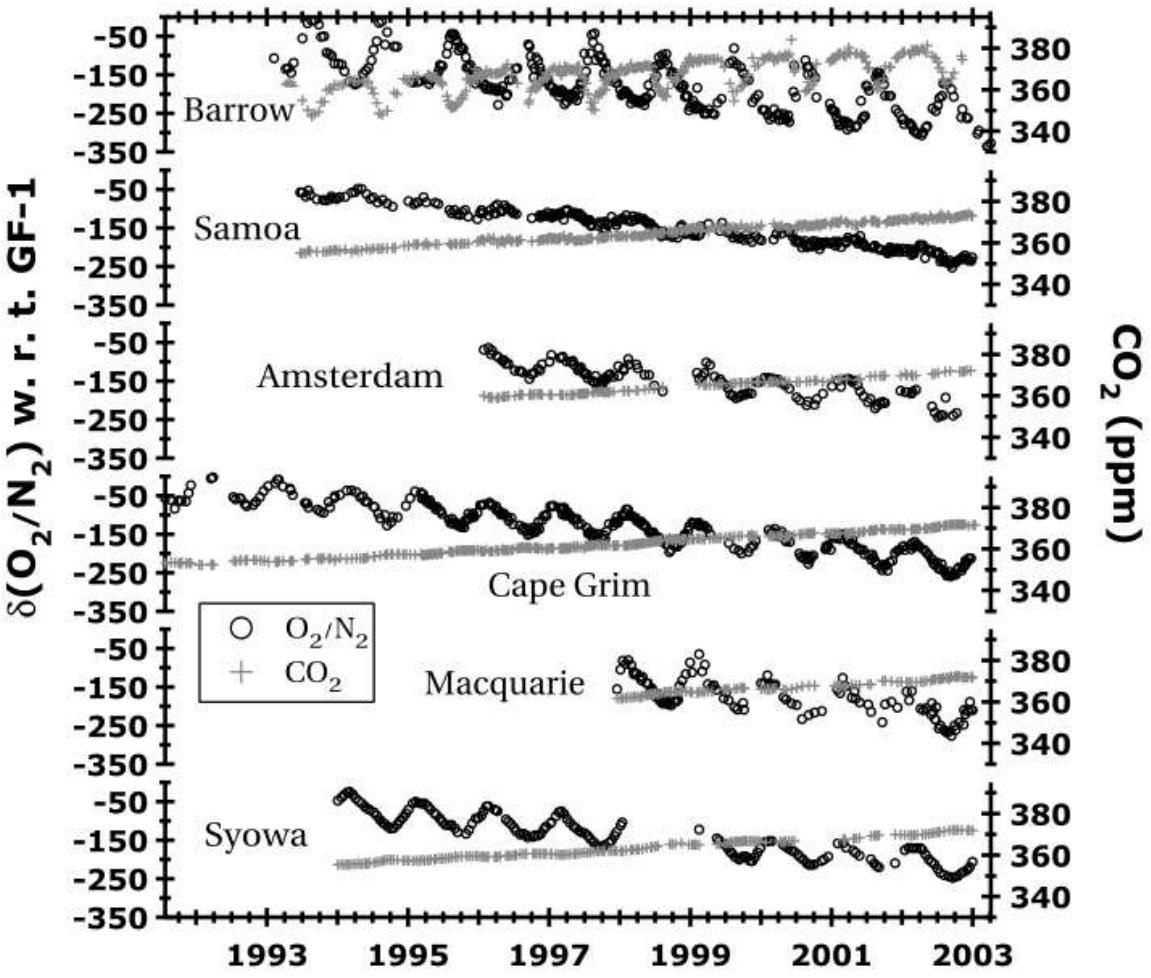

Figure 2. O_2/N_2 and CO_2 records between 1991-2003. The CO_2 data show expected features: anthropogenic increase, and a seasonal cycle, harder to see in the sites of the southern hemisphere, attributed to terrestrial biomass. Calculated with [eq-1] using GF-1 as the reference gas, the O_2/N_2 data show a long term decrease due to O_2 consumption during combustion, although smaller than this consumption. This difference is mostly due to terrestrial photosynthetic O_2 production. There is also a small contribution of O_2 from ocean degassing linked to increased temperatures. The O_2/N_2 data also show a seasonal cycle, which is the result of adding the land and ocean contributions. [*Bender et al.*, 2005]

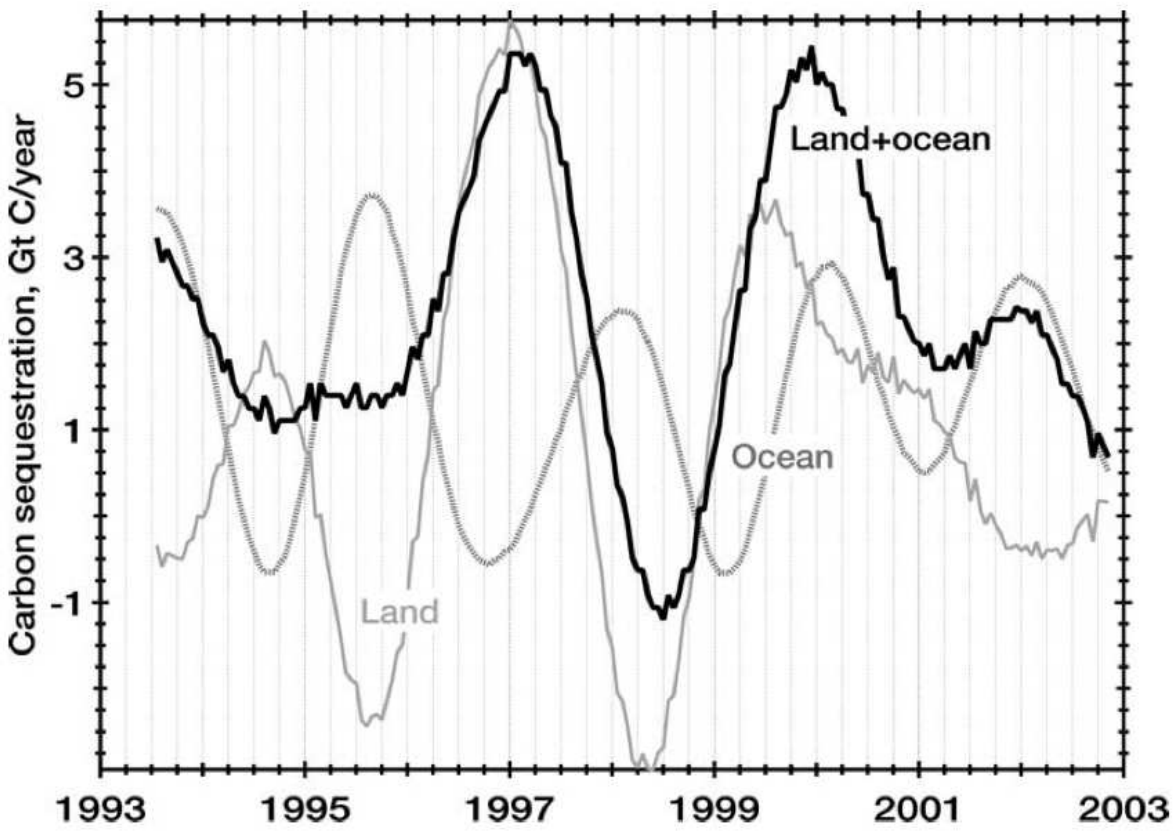

Figure 3. Global land and ocean CO_2 sequestration rates calculated from $\delta(O_2/N_2)$ and CO_2 data for Barrow, Samoa and Cape Grim sites only because they have the longest and most reliable records. The ocean sink seems to be smoother and less variable than the land sink. CO_2 sequestration rates for the land biosphere covary closely with total sequestration rates from 1996-2001, except for the decrease in land sequestration in 1999 for 6 months. The rapidly decreasing sequestration rate in 1997-1998 is attributed to a strong El Niño event and is believed to be caused by increased aridity and biomass burning. During El Niño, an anti-correlation between ocean and land sink is expected, however there is no known explanation for this out-of-phase behavior during periods of no El Niño. There are periods of time when both the ocean and land are sources and not sinks of CO2. [*Bender et al.*, 2005]

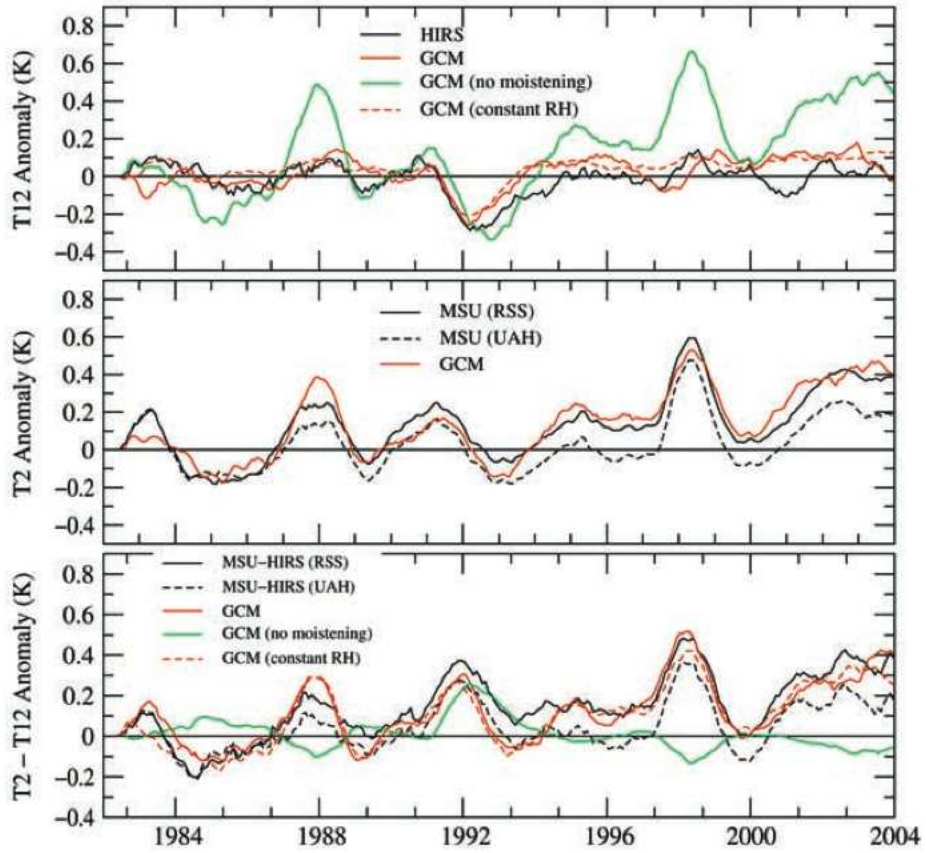

Figure 4. Global mean time series of T12 (top), T2 (middle), and $T2-T12$ (bottom) from GCM simulations (red) and satellite observations (black). The T12 channel corresponds to the HIRS, which quantifies both changes in temperature and water vapor. The T2 channel corresponds to the MSU, which quantifies only changes in temperature. The difference between the 2 channels is shown in the bottom graph, which represents only changes in water vapor. The model-simulated radiances are also shown from calculations using a seasonally varying climatological profile with no moistening trend [green line] and a prescribed moisture profile that moistens at a constant relative humidity rate [red dashed line]. Notice that the GCM simulation that maintains constant relative humidity predicts the observed change in upper tropospheric water vapor very well. All time series are smoothed with a 6-month running mean. [*Soden et al.*, 2005]

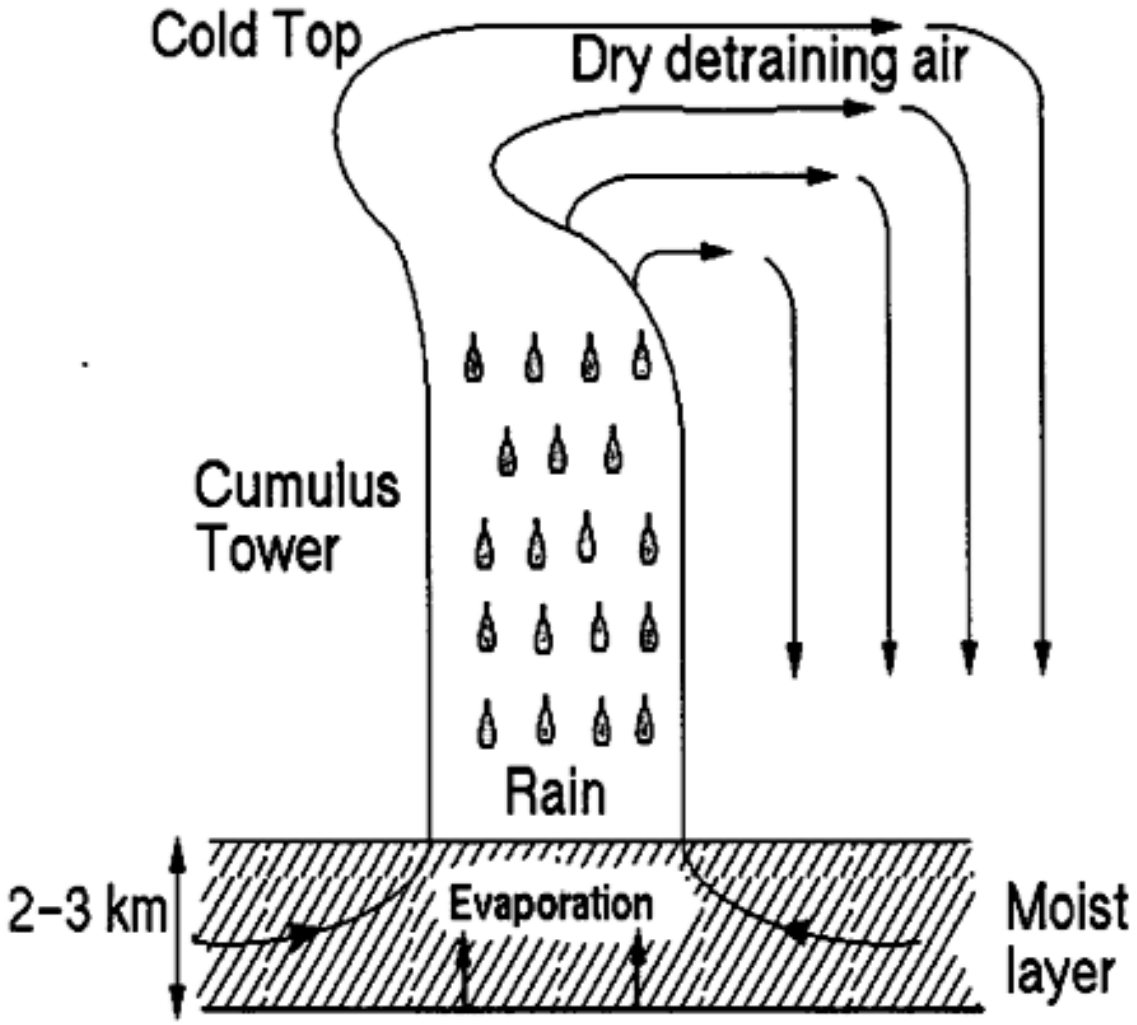

Figure 5. An illustration of Lindzen's theory. A cumulus tower created by moisture evaporated from the surface that is later rained out, leaving the air parcel to detrain. This creates a drier atmosphere at altitudes above 5km. This theory was later disproven by Soden *et al.*in 2005. [*Lindzen*, 1990]

Model 1. *Calculation of CO_2 sinks by Bender* et al. *[2005]*

Having the concentration of $\delta(O_2/N_2)$ and the CO_2 as a function of time (from Fig 2), it is straightforward to compute the ocean and land sinks using the following two equations:

$$f_{ocean} = -\frac{\alpha_{bio} - \alpha_{fuel}}{\alpha_{bio}} f_{fuel} - f_{cement} - \frac{1}{\beta\gamma\alpha_{bio}} \frac{d(\delta(O_2/N_2) + \gamma\alpha_{bio} CO_2)}{dt}. \quad (2)$$

$$f_{land} = -f_{fuel} - f_{cement} - f_{ocean} - \frac{1}{\beta}\frac{dCO_2}{dt} \quad (3)$$

where f are fluxes of CO_2 with the convention that negative means a source to the atmosphere, α is an average molar exchange, and β and γ are conversion factors [*Bender et al.*, 2005]. α_{bio} and α_{fuel} are the mean changes in O_2/CO_2 during photosynthesis and fuel combustion respectively. The fluxes of fossil fuel and cement are taken from [*Marland et al.*, 2003]. The values of specific constants are given in Table 1. Once values for f_{ocean} and f_{land} were obtained, Bender *et al.* [2005] corrected them for an estimated 0.3 Gt C/yr O_2 outgassing from the oceans.

Uncertainties in these calculated sinks come from: analytical errors, limited O_2 and CO_2 sampling, uncertainties in air-sea O_2 exchange including O_2 outgassing, uncertainties in fossil fuel combustion rates, and uncertainties in α_{bio}.

Table 1. Conversion factors and other terms for calculation the anthropogenic CO_2 balance (from [*Bender et al.*, 2005])

Symbol	Description	Value	Units
β	Gt C to ppm CO_2	0.471	ppm/Gt C
γ	ppm O_2 to per meg $\delta(O_2/N_2)$	4.8	per meg/ppm
α_{fuel}	mean change in O_2/CO_2 during combustion	-1.45	
α_{bio}	mean change in O_2/CO_2 during photosynthesis	-1.1	
f_{fuel}	fuel of CO_2 due to fossil fuel combustion	variable in time(avg. 6.26)	Gt C/yr
f_{cement}	flux of CO_2 due to cement manufacturing	variable in time(avg. 0.21)	Gt C/yr

History of Black-Body Radiation

Jonathan D. Bent

Scripps Institution of Oceanography, University of California, San Diego, USA

Stéphanie d'Agata

Scripps Institution of Oceanography, University of California, San Diego, USA

Sandra E. Kirtland

Scripps Institution of Oceanography, University of California, San Diego, USA

1. Abstract

This paper will present a brief history of the black-body radiation laws. Concentration is on the work of five individuals: Gustav Kirchhoff, Josef Stefan and Ludwig Boltzmann, Wilhelm Wien, and Max Planck. Each of these theorists attempted to describe the same observed physical phenomenon. The focus of this paper is on the theoretical and mathematical derivation of their different laws.

2. Introduction

Development of the black-body laws was a major step in understanding radiation. In 1865 James Clerk Maxwell was the first scientist to propose both that a changing magnetic field causes an electric current and that an electric current generates a magnetic field. The wave resulting from these simultaneously changing fields is an electromagnetic wave, moving at the speed of light (Strobel, 2001). By the mid-19th century, scientists had realized that all objects at some temperature above absolute zero emit light and heat, which they identified as examples of electromagnetic radiation, with the amount of radiation emitted by a given body depending on its unique composition (Fowler, 1997). In order to better understand the nature of radiation emitted by bodies, Gustav Kirchhoff developed the concept of a black-body in 1862. This theoretical body could absorb all radiation incident upon it; thus, it could also emit the maximum amount of radiation at any temperature and wavelength. Kirchhoff measured the thermal spectra for a black-body at different temperatures—demonstrating the dependence of the intensity of radiation emitted at a given wavelength on temperature (Strobel, 2001). Following Kirchhoff's experimental results, a number of scientists attempted to formulate a mathematical relationship for the dependence of irradiance on temperature and wavelength (or frequency). After a brief

description of Kirchhoff's experiment, this paper will focus on the work of these scientists to accurately model observed thermal spectra.

3. Kirchhoff's Development of the 'Black-body' Concept

Gustav Kirchhoff developed the concept of a black-body, which was fundamental to understanding the nature of radiation. Kirchhoff focused his thermodynamic studies on patterns of emission and absorption of radiation by heated gases, liquids and solids. In 1859, Kirchhoff conducted an experiment that examined the emission of radiation from cavities within several bodies of different material, size and shape (Kuhn, 1978). No object can be a perfect emitter, so Kirchhoff used the principle of cavity radiation, which suggests that almost all radiation incident upon a small heated cavity is absorbed due to the large number of reflections it undergoes inside the cavity, with some radiation absorbed by the material at each reflection (cavity is perfectly reflecting) (Sell and Walsh, 2002). He concluded that the ratio of absorbed radiation to emitted radiation was a function only of the temperature of the body and the wavelength of emission. He formulated his finding through the following relationship (Kuhn, 1978):

$$e_\lambda/a_\lambda=K_\lambda(T) \quad (1)$$

where e_λ is the emission at a particular infinitesimal wavelength, a_λ is the absorptivity at a particular infinitesimal wavelength, and K_λ is a distribution function of radiation intensity based on temperature T and wavelength λ. In a black-body, where all incident radiation is absorbed, absorption equals emission.

4. Stefan-Boltzmann's Law for the Temperature Dependence of Irradiance

Josef Stefan and Ludwig Boltzmann attempted to quantify the relationship demonstrated by Kirchhoff's data that the irradiance of a body depends on its temperature. Their result was a formula for the dependence of total irradiance on temperature and did not describe differences in irradiance with wavelength. Observing thermal spectra for a black-body (see Figure 1), Stefan noticed an exponential increase in irradiance with temperature. He determined that the dependence of irradiance on the fourth power of temperature produced graphs that best approximated the data. At the same time, Boltzmann derived this result mathematically. To obtain an expression for the dependence of irradiance on temperature, Boltzmann assumed that irradiance must be related to energy density u by $u = 4\pi K_\lambda/c$, where K_λ is the distribution function of irradiance developed by Kirchhoff and c is the speed of light. He held that this assumption was necessary to maintain thermal equilibrium. Based on equation (1), total energy density must be a function of temperature alone. Treating radiation as a wave allowed Boltzmann to apply a previous discovery that each incident wave would exert a pressure related to its energy density by $p = u/3$. Boltzmann described a scenario in which the black-body radiation does work to expand the cavity. In this case, an input of heat is required to maintain thermal equilibrium. Using the first and second laws of thermodynamics, he was able to derive the result that $du/u = 4\ dT/T$ (Sturge, 2003). Through this derivation and experimental data, Boltzmann determined the value for the constant of proportionality, $\sigma = 56.7$ nW m^{-2} K^{-4} (Atkins, 2002). Combining Stefan and Boltzmann's findings yielded the following relationship, published in 1879 (Kuhn, 1978):

$$F^* = \sigma T^4 \qquad (2)$$

5. Wien's Laws

Continued observations of the thermal spectra of black bodies by André Crova, Samuel Langley, and others, led to the conclusion that maximum emission occurs at a shorter wavelength when the black-body is at a higher temperature (Kangro, 1976). In 1893 Wilhelm Wien published a formula attempting to describe this displacement of maximum irradiance (Atkins, 2002). He started with the Stefan-Boltzmann law for total radiation and proposed extending these conclusions to radiation split up into separate wavelengths.

Wien used many of the same techniques as Boltzmann, also considering the case of radiation doing expansion work on a cavity. He represented this as a cylinder closed by a piston, both perfectly reflecting in order to conserve the total energy of radiation inside the cylinder. His goal was to observe the distribution of energy among all wavelengths of radiation inside the cylinder during an adiabatic expansion. To do so, he applied the Doppler effect (see Figure 2)—which describes the apparent change in frequency and wavelength perceived by an observer moving relative to the source of the wave—since expansion of the cylinder was equivalent to a moving observer. During expansion, there was a relative increase in frequency of radiation at the piston and a decrease in frequency of radiation inside the cylinder. This led to a re-distribution of energy towards longer wavelengths inside the cylinder as temperature decreased because $\lambda = c/\nu$ (Kuhn, 1978).

Wien then used the second law of thermodynamics to quantify this redistribution of energy. He found entropy S to be a function of internal energy U divided by frequency ν, related this function to temperature by $dS/dU = 1/T$, and related energy density and total energy by $u=(8\pi\nu^2)U/(c^3)$. Wien thus arrived at a formula for energy density called the displacement law (Kuhn, 1978):

$$u_\lambda = 1/\lambda^5 \, \phi(\lambda T) \qquad (3)$$

where $\phi(\lambda T)$ represented some function of a single variable, equivalent to Kirchhoff's distribution function of radiation K_λ from equation (1). After continued derivation, based partly on the work of contemporary physicists H. F. Weber and Friedrich Paschen, Wien represented the distribution function as:

$$K_\lambda = (b/\lambda^5)\,(1/e^{a/\lambda T}) \qquad (4)$$

Wien published this law in 1896, representing the movement of maximum irradiance to shorter wavelength with an increase in temperature (Kuhn, 1978). Wien applied his laws to experimental spectra data to achieve the result (Curry and Webster, 1999):

$$\lambda_{max} = 2897.8 / T \qquad (5)$$

6. Planck's Law of Black-body Radiation

While Wien's formula matched observed thermal spectra at short wavelengths, it deviated from experimental data at long wavelengths. During the early 20th century, Max Planck developed a law to correct these errors. Planck agreed with Wien's use of an expression for entropy to formulate a relationship between energy density (proportional to irradiance), temperature, and wavelength; he simply disagreed with the particular expression for entropy that Wien used. Thus, Planck's primary goal was to find S=f(U) in a different form than that used by Wien.

Planck began by considering that the emission of radiation from a black-body could be distributed among tiny charged "oscillators" present in the matter. Planck defined the energy U of a single oscillator as an ensemble average of N identical oscillators so that the total energy U_N of a system of oscillators would be equal to NU. U_N was dividable into an integral number of elements ε of energy because the black-body contained an integral number of oscillators. These

oscillators Planck described were actually atoms; he was simply stating there must be an integral number of these elements within matter. Next Planck formulated an expression for R, the number of possible distributions of the energy elements over all N oscillators. Equating this expression to entropy using a formula earlier derived by Boltzmann that $S_N=k \log R$ where k is a constant, Planck derived the following expression for entropy (Planck, 1901):

$$S=k\{(1+U/\varepsilon)\log(1+U/\varepsilon)-U/\varepsilon\log(U/\varepsilon)\} \qquad (6)$$

Once Planck had developed a different equation for entropy based on his use of an ensemble average of oscillators, he was able to obtain an expression for ε, $\varepsilon=h\nu$ with h as a constant, by applying Wien's equation for entropy $S=f(U/\nu)$. With entropy now in terms of hν, Planck differentiated his expression with respect to U and applied the relation $dS/dU=1/T$ and $u=(8\pi\nu^2)U/(c^3)$ (just as Wien did with his expression for entropy) in order to find his final expression for energy density in terms of wavelength, which he then related to irradiance:

$$F^*=\{8\pi hc/\lambda^5\}\{1/(e^{hc/\lambda kT}-1)\} \qquad (7)$$

Planck's law fit data for spectral energy density at all wavelengths (Planck, 1901).

7. Conclusion

Kirchhoff's major discovery in 1859—that a black-body absorbs all incident energy and re-radiates the maximum amount of energy for any given temperature and wavelength—led a number of scientists to work on mathematical explanations for his observations. Stefan, Boltzmann, and Wien attempted to describe various aspects of thermal spectra, including the temperature dependence of irradiance and the displacement of maximum irradiance towards shorter wavelength with an increase in temperature. However, it was Planck who discovered the comprehensive equation for black-body radiation in 1901. As a mathematical technique in

deriving his equation, Planck proposed describing the total energy in matter as an integral sum of indistinguishable energy elements called quanta. Five years later, Einstein applied this interpretation of energy to a beam of light in order to describe the absorption and emission of light by matter, known as the photoelectric effect (Atkins, 2002). This new understanding of electromagnetic radiation was the precursor to the replacement of classical electromagnetism with quantum mechanics. Planck, without knowing it, had discovered the underlying assumption of quantum theory.

8. Annex

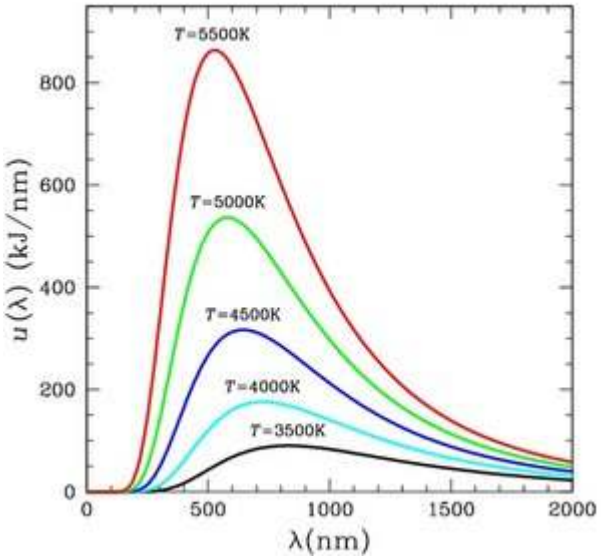

Figure 1: Thermal spectra for a black-body. Displays the spectral intensity of electromagnetic radiation at all wavelengths from a black-body at temperature T. (Wikipedia)

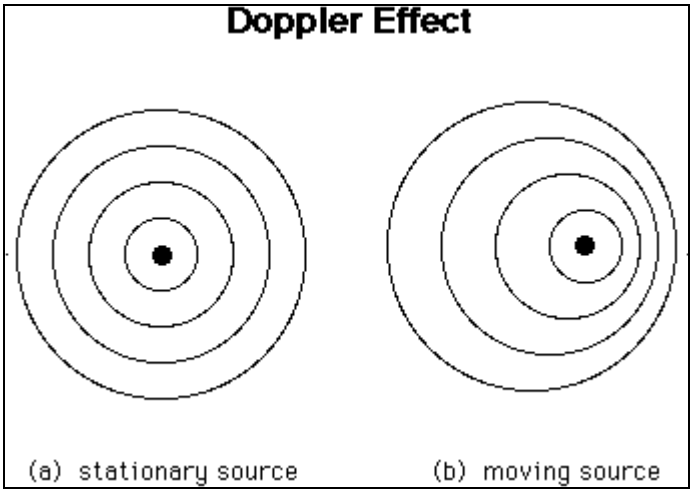

Figure 2: The Doppler effect (Wikipedia)

8. References

Atkins, P. and Paula, J, 2002: Physical Chemistry. 7th ed. W.H. Freeman and Co, NY. pg. 294 -295.

Curry J.A and Webster P.J, 1999: Thermodynamics of Atmospheres and Oceans. *Academic Press, San Diego.*

Fowler, M., 1997: "Black-body Radiation." *University of Virginia*. Available at http://galileo.phys.virginia.edu/classes/252/black_body_radiation.html

Kangro, H., 1976: Early history of Planck's radiation law. *Tailor and Francis LTD*.

Kuhn T.S., 1978: Black-body theory and the quantum discontinuity. *Clarendon Press, Oxford. Oxford University Press, New York.*

Planck, M., 1901: On the Law of Distribution of Energy in the Normal Spectrum. *Annalen der Physik.* vol. 4, p. 553. 1901. Available at http://en.wikipedia.org/siki/Planck's_las_of_black_body_radition

Sell, H.G. and Walsh J.P, 2002: Heat radiation. *Access Science-McGraw Hill*. http://www.accessscience.com, DOI 10.1036/1097-8542.311000

Strobel, N., 2001: Electric and Magnetic Fields. Available at http://www.astronomynotes.com/light/s2.htm

Sturge, M.D., 2003: Statistical and Thermal Physics. *AK Peters, Natick, Massachusetts*. pg. 206 -207.

Recent Advances in Understanding Earth's Radiation Budget

Jonathan D. Bent

Scripps Institution of Oceanography, University of California, San Diego, USA

Stéphanie d'Agata

Scripps Institution of Oceanography, University of California, San Diego, USA

Sandra E. Kirtland

Scripps Institution of Oceanography, University of California, San Diego, USA

1. Abstract

This paper will discuss recent advances in our understanding of the overall radiation budget of the Earth. First, the combination of satellite measurements with calculations for surface radiation using parameterizations allowed the quantification of clouds' impact on short wave and long wave radiation fluxes. Next, recent attempts have been made to isolate the influence of feedbacks on the affect of greenhouse gas forcing on long wave radiation. Understanding how these factors affect Earth's radiation budget is critical for modeling climate change.

2. Introduction

Variable short wave solar radiation is the driving force for Earth's climate (Crowley and Kim, 1994). In addition to incident short wave (SW) radiation, the Earth acts as an approximate black body, emitting long wave (LW) radiation. Simple climate models show how the balance between incoming and outgoing radiation roughly determines Earth's temperature. However, the addition of an atmosphere alters Earth's radiation budget (Lindzen and Emanuel, 2005).

The net effect of clouds is a balance between a warming effect through decreasing outgoing LW radiation and a cooling effect through decreasing incoming SW radiation (Wielicki et al., 2002). Most studies on the affect of clouds on Earth's climate have related to the role of total cloud cover, rather than cloud-type variations, on the distribution of solar radiation (Chen et al., 1999). Advances in cloud microphysics have led to the conclusion that cloud radiative properties differ based on the clouds' microphysical constitutions (relative amount of liquid water and ice). Section 3 of this paper will address the work of Tian and Ramanathan (2002) to isolate the role of three main cloud types in the net cloud radiative forcing (CRF) of the tropical Pacific.

Researchers have long understood the role of the greenhouse gases in trapping and re-radiating LW radiation back to the Earth's surface. The increase of CO_2 in the atmosphere has amplified this effect, decreasing the amount of LW radiation lost to space, but feedbacks due to clouds and water vapor make it difficult to isolate the impact of greenhouse gas forcing. Section 4 will describe work by Philipona et al. (2005) to quantitatively separate the radiative forcing due to greenhouse gas forcing from that due to a positive water vapor feedback. Accounting for atmospheric effects on Earth's radiation budget is critical for understanding changing climate.

3. Effect of clouds on Earth's radiation budget

The three main cloud types studied by Tian and Ramanathan are the high clouds, middle clouds, and low clouds. These clouds are characterized by differences in temperature, altitude, and microphysics. Tian and Ramanathan evaluated the role of the various cloud types using measurements of CRF, which is the difference between the cloudy and clear sky convergence of radiant flux in a volume, measured in Wm^{-2} (Mace et al., 2006). The reason for evaluating clouds in the tropical Pacific was the availability of energy budget data from the period 1985-1989 using the Tropical Ocean Global Atmosphere Coupled Ocean-Atmosphere Response Experiment and the Central Equatorial Pacific Experiment. The study used top of the atmosphere (TOA) radiation data from three satellites (NASA and NOAA) provided by the Earth Radiative Budget Experiment (ERBE) and calculated radiation at the surface and within the atmosphere using empirical parameterizations derived from radiation models and observational data from the aforementioned experiments by Li and Leighton (1993) and Inamdar and Ramanathan (1994) (for more details on procedure, see Tian and Ramanathan, 2002).

3.1 The high clouds

Located above 440mb, high clouds consist of cirrus, cirrostratus, and deep convective clouds, with more than 25% located in moist convective regions (Tian and Ramanathan, 2002). Due to the existence of large ice crystals, cirrus clouds strongly absorb LW radiation and re-emit it back to the surface, with some passing through the TOA (Smith et al., 1998). Without high clouds, the temperature at the TOA would be colder; therefore, cirrus clouds have a positive LW CRF effect at the TOA with an average value of 35 Wm^{-2} (see Figure 1 for a visual representation of high cloud amount and LW fluxes) (Tian and Ramanathan, 2002). However, large SW CRF largely cancels the TOA warming by LW radiation, especially when clouds contain small ice crystals on the order of a few micrometers in diameter, since these cause a particularly high albedo (Liou, 2005). Within the atmosphere, high clouds exert a LW CRF equal to approximately 50 Wm^{-2} because of the high amount of water vapour, resulting in warming. In addition there is absorption of SW in the atmosphere equal to 20 Wm^{-2}. This high absorption of radiation in the atmosphere means that LW fluxes have a weak effect at the surface. Thus, the negative SW CRF due to albedo dominates, and high clouds cause net cooling effect at the surface.

3.2 The low clouds

Located below 680mb, low clouds consist of stratus, stratocumulus, and cumulus clouds, with over 30% occurring over cold oceans with lower than average sea surface temperatures (<25°C) (Tian and Ramanathan, 2002). Low clouds have a cloud top temperature similar to surface temperature, so they radiate at the same wavelength as the Earth, and as a consequence, LW CRF at the TOA due to low clouds is indistinguishable (Tian and Ramanathan, 2002; Chen et al., 1999). The high reflectivity of low clouds causes high SW CRF at the TOA and within the

atmosphere, resulting in radiative cooling with an average value of -20 Wm^{-2} (see Figure 2 for a visual representation of low cloud amount and LW fluxes). The reflectance of clouds increases with the increase of the liquid water path and the decrease of droplet radius (smaller cloud droplets absorb less solar radiation and increase the reflectance of the cloud) (Ackermann et al., 1986). The surface absorbs downward LW fluxes because there is little moisture below low clouds, but negative SW CRF due to reflectivity causes net cooling.

3.3 Summary of cloud effects

Overall, high clouds dominate the warming effect and low clouds dominate the cooling effect. Middle clouds have much less impact, but are shown to cause a slight cooling at the surface and a slight warming within the atmosphere (Tian and Ramanathan, 2002). For a summary of cloud effects see Table 1. See Figure 3 for a spatial representation of net CRF in the Tropical Pacific for each layer of the atmosphere.

4. Effect of anthropogenic greenhouse gas forcing and the water vapor feedback on LW radiation

A recent study by Philipona et al. (2005) aimed to separate the relative importance of different feedbacks from greenhouse gas forcing on Earth's radiation budget. The study was an attempt to explain the monthly land-based average surface temperature measurements in the crutem2 dataset generated by the University of East Anglia's Climate Research Group. This data demonstrated significant warming in Europe over the last 25 years and a distinct warming gradient from East to West, in terms of a change in radiative forcing (Jones and Moberg, 2003). They attributed this gradient to the non-uniform distribution of water vapor, which would

amplify greenhouse gas-induced warming if there was a positive water vapor feedback. With a positive feedback, warm air will re-radiate more heat than cold air, so an increase in the water vapor content of the atmosphere and the transport of this water vapor to high, cold altitudes will decrease the amount of LW radiation lost to space (Del Genio, 2002). In order to understand the relative importance of greenhouse gas forcing and other feedbacks on warming, this study correlated crutem2 temperature data and ERA-40 relative humidity data from the European Center for Medium Range Weather Forecasts with measurements of radiative forcing from the Alpine Surface Radiation Budget (ASRB) network.

Philipona et al. (2005) found a strong correlation (R^2 = .99) between temperature change and changes in the flux of LW downward radiation (LDR) for cloud-free situations. The authors asserted that the observed increase in LDR was due to increasing surface temperature and increasing water vapor content of the atmosphere. Using the first derivative of the Stefan Boltzmann law, the authors determined the relative contribution to LDR by increased surface temperature. They subtracted this from the overall annual LDR value and found a value of +1.18 Wm^{-2} for cloud-free, temperature independent LDR. The use of sensitivity values for the dependence of LDR on water vapor allowed the authors to extract a value of +0.35 Wm^{-2} for forcing by anthropogenic greenhouse gases, leaving a value of +.83 for radiative forcing due to the water vapor feedback. This data demonstrated that the positive water vapor feedback more than doubled anthropogenic greenhouse gas forcing of LDR (Philipona et al., 2005).

5. Conclusion

Recent advances have demonstrated the importance of clouds and greenhouse gases on Earth's radiative budget. Measurements by Tian and Ramanathan (2002) on the role of cloud type on

radiative forcing demonstrate that low-level clouds increase albedo significantly, while high clouds play a large role in trapping and re-radiating heat. Additionally the study by Philipona et al. (2005) separated the radiative forcing due to greenhouse gases from the forcing due to the water vapor feedback, providing strong evidence for a positive water vapor feedback. Together, greenhouse gas forcing and its associated feedbacks have resulted in a strong increase in LDR. These new discoveries are extremely important for improving global climate models. Results have increased confidence in the accuracy of the water vapor feedback in global climate models and may help with the parameterization of cloud effects, which remain the models' weakest component (Stephens, 2005).

6. Annex

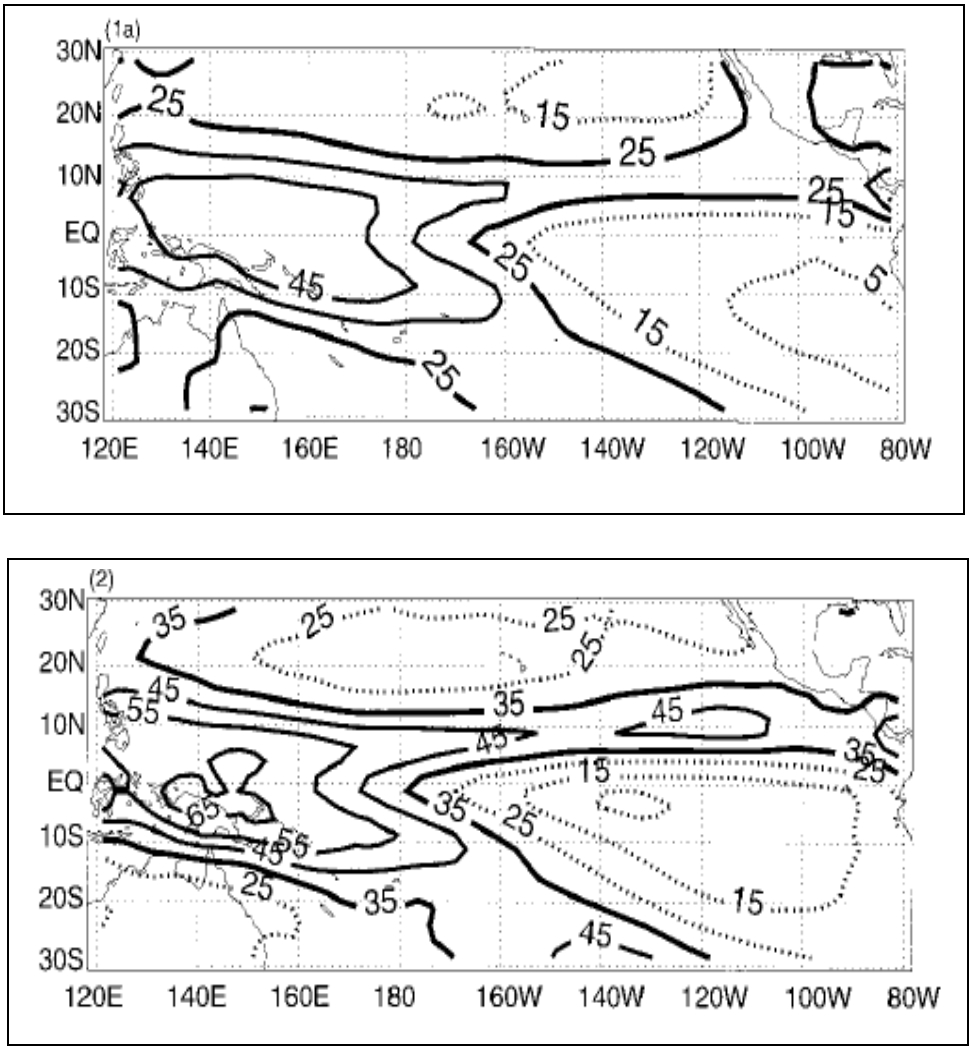

Figure 1: Annual mean high cloud amount (top) and Annual-mean LW CRF at the TOA from ERBE (Wm^{-2}) demonstrating a correlation between high cloud amount and LW CRF at the TOA (bottom) (Tian and Ramanatha, 2002).

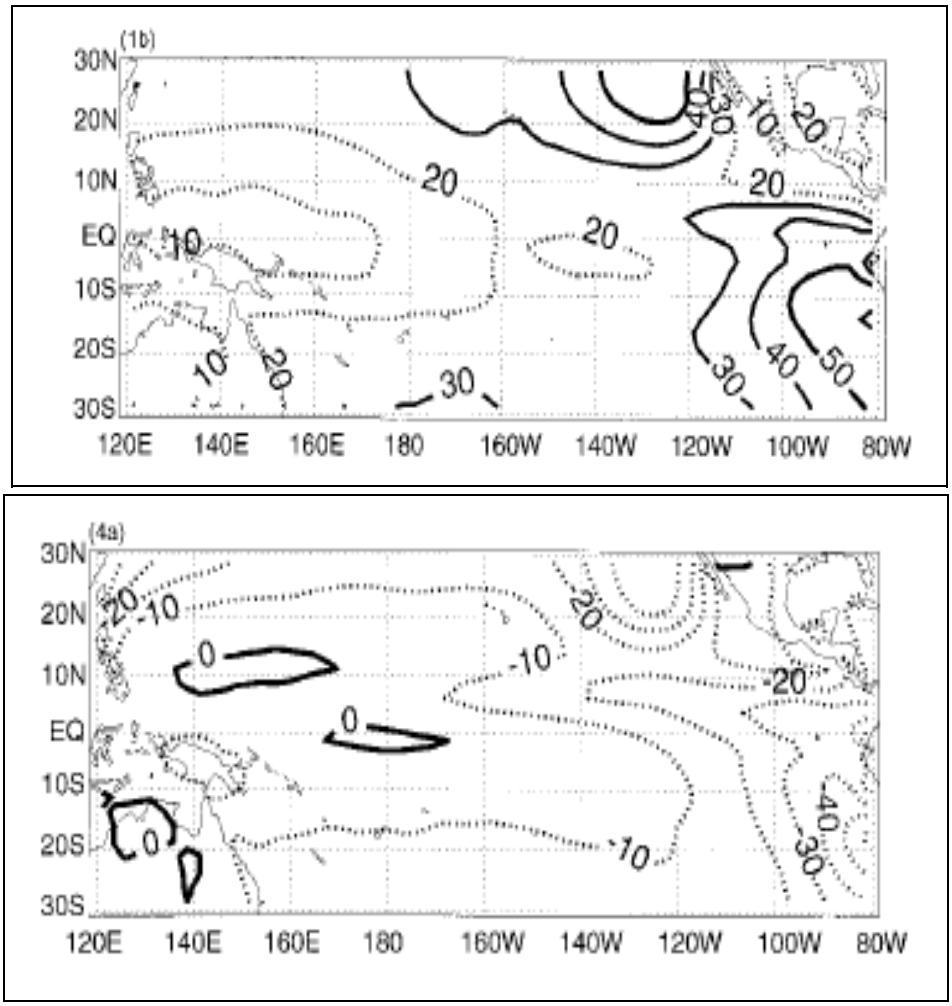

Figure 2: Annual mean low cloud amount (top) and Annual-mean net CRF at the TOA from ERBE (Wm^{-2}) demonstrating a correlation between low cloud amount and net CRF at the TOA (bottom) (Tian and Ramanathan, 2002).

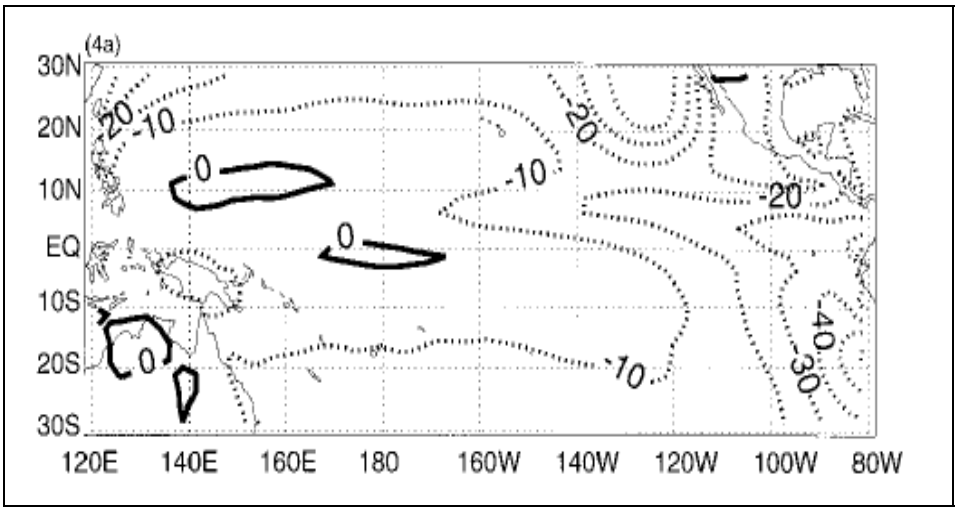

(a)

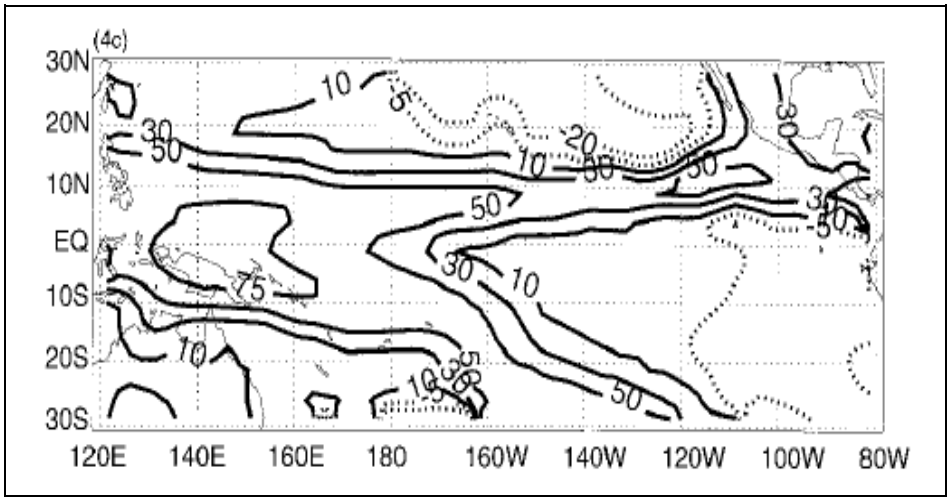

(b)

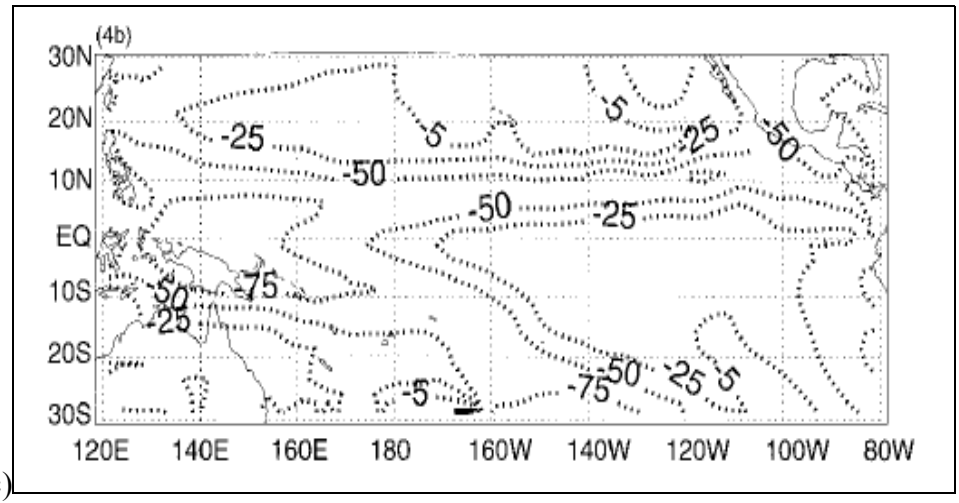

(c)

Figure 3: Net CRF (Wm^{-2}): (a) at the TOA, (b) in the atmosphere, and (c) at the surface (Tian and Ramanathan, 2002).

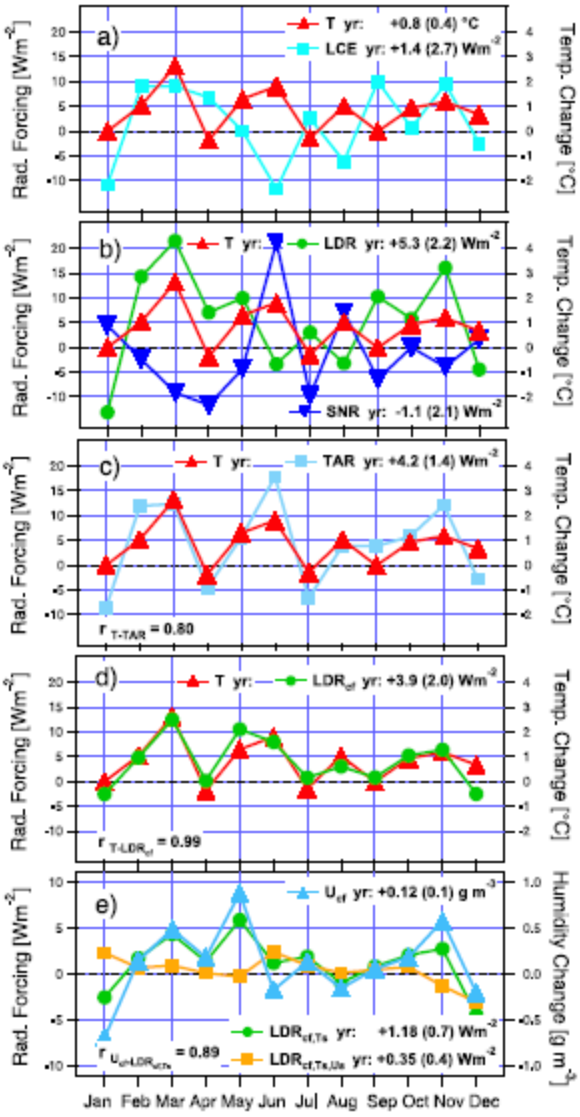

Figure 4: Describes monthly changes in temperature, relative humidity, and radiative forcing over the period 1995-2002 in the Alps. a) Correlates changes in the LW cloud effect with changes in temperature. b) Correlates changes in LDR and changes in SW net radiation with changes in temperature. c) Correlates change in total absorbed radiation with changes in temperature. d) Correlates changes in LDR in cloud-free scenarios with changes in temperature. e) Correlates changes in LDR in cloud free scenarios where the temperature effect is subtracted and changes in LDR in cloud free scenarios where the temperature and humidity effects have been subtracted with changes in total humidity in cloud free scenarios.

Table 1 : Summary of the relative contributions of the clouds to Net Cloud Radiative Forcing (NetCRF), for the TOA, the atmosphere, and the surface. Values are taken from Tian and Ramanathan (2002).

	Low Clouds	***Middle Clouds***	***High Clouds***
Top Of the Atmosphere	- because of the temperature of the top of the clouds, low contribution to LW CRF ➔ LW CRF ~ 25Wm^{-2}	➔ LW CRF ≈ 30 Wm^{-2}	- High clouds absorb OLR: high reemission if IR. ➔ LW CRF > 35Wm^{-2}
	- because of their strong albedo, clouds have a net cooling effect ➔ SW CRF << 0 Wm^{-2}		Solar albedo ≈ IR greenhouse effect ➔ SW CRF = LW CRF
	➔Net Low Cloud CRF < 0 Wm^{-2}		➔Net High Cloud CRF ≈ 0Wm^{-2}
Inner-Atmosphere	- because of their low absorptivity and their high reflectivity, less LW is emitted to the atmosphere. Therefore, they exert a cooling effect on the atmosphere: ➔ LW CRF ≈ -20Wm^{-2}	↑ **MIDDLE CLOUDS** ↓	↑ HIGH CLOUDS ↓ - *Absorption IR by water vapor:* ➔ high LW CRF ≈ 50Wm^{-2}
	➔ SW CRF ≈ 0Wm^{-2}		- large cloud solar absorption ➔ SW CRF ≈ 20Wm^{-2}
	➔ Net Low Cloud CRF ≈ -20Wm^{-2} ↑ **LOW CLOUDS** ↓	➔ LW CRF ≈ 30 Wm^{-2} Net LW ≈ 0 Wm^{-2} - Seems to have a slight warming effect	➔Net High Cloud CRF ≈70 Wm^{-2}
Surface	- low LW CRF ➔ weak positive effect		because a large part of LW CRF is absorbed by the atmosphere: ➔ weak LW CRF
	- Strong Albedo of the low clouds creates a cooling effect. ➔ negative SW CRF		- because of their albedo, less SW radiation reach the surface: ➔ negative SW CRF but weaker than for low clouds.
	- Because LW CRF << SW CRF: ➔Net low cloud CRF ≈ -20 Wm^{-2}	Net cooling effect	➔ Net high cloud CRF <0 W m^{-2}

7. References

Ackermann, S.A., and G. L Stephens, 1986: Absorption of Solar Radiation by Cloud Droplets: An Application of Anomalous Diffraction Theory, *Journal of Atmospheric Sciences, Vol 44, No. 12*

Chen T., Rossow W.B., Zhang Y., 1999: Radiative Effects of Cloud-Type Variations. *Journal of Climate, volume 13.*

Crowley, T., and K. Kim, 1994: Milankovitch Forcing of the Last Interglacial Sea Level.*Science*, *265*: *1566-1567.*

Del Genio, A. D., 2002: The Dust Settles on Water Vapor Feedback. *Science, 296*: *665 666.*

Hartmann D.L., Ockert-Bell M.E., and Michelsen M.L., 1992: The effect of cloud type on earth's energy balance : Global analysis. *Journal of Climate, 5: 1281-1304.*

Inamdar, A.K, and V. Ramanathan, 1994 : Physics of greehouse effect and convection in warm oceans. *Journal of Climate,* **7**, 715-731.

Jones, P. D., and A. Moberg, 2003: Hemispheric and large-scale surface air temperature variations: An extensive revision and an update to 2001. *Journal of Climate, 16*: *206 223.*

Li W.T, and H.G. Leighton, 1993 : Global Climatologies of Solar Radiation budget at the surface and in the atmosphere from 5 years of ERBE data. *Journal of Geophysical Research,* **98**, 4919-4930.

Lindzen, R. S., and K. Emanuel, 2002: The greenhouse effect. Encyclopedia of Global Change, Environmental Change and Human Society, Vol. 1 (A. S. Goudie, ed.). New York: Oxford University Press, pg. 562-566.

Liou K.N, 2005: Yearbook 2005. Found at http://www.atmos.ucla.edu/~liougst/Group_Papers/

Mace G.G, Benson S and Kato S, 2006: Cloud Radiative forcing at the Atmospheric Radiation Measurement Program Climate Research Facility: 2. Vertical Distribution of radiant energy by clouds. *Journal Of Geophysical Research, Vol.111, D11S91, doi: 10.1029/2005JD005922,2006.*

Petty G.W., 1958: A First Course in Atmospheric Radiation. *Sundog Publishing G, Madison, Wisconsin*

Philipona, R., Durr, B., Ohmura, A. and C. Ruckstuhl, 2005: Anthropogenic greenhouse forcing and strong water vapor feedback increase temperature in Europe. *Geophysical Research Letters, 32: L19809, doi:10.1029/2005GL023624.*

Smith W.L, Ackermann S, Revercomb H., Huang H., DeSlover D.H, Feltz W., Gumley L. and Collard A., 1998: Infrared spectral absorption of nearly invisible cirrus clouds. *Geophysical Research Letters, Vol. 25, No. 8, Pages 1137-1140*.

Stephens, G. L., 2005: Cloud feedbacks in the climate system: A critical review. *Journal of Climate. Vol. 18 (2): 237-273.*

Tian, B. and V. Ramanathan,2002: Role of Tropical Clouds in Surface and Atmospheric Energy Budget. *Journal Of Climate, Vol 15: 296-305.*

Wielicki, B.A., Wong, T., Allan, R.P, Slingo, A., Kiehl, J.T., Soden, B.J, Gordon, C.T., Miller, A.J., Yang, S., Randall, D.A., Robertson, S., Susskind, J., and H. Jacobowitz, 2002. Evidence for Large Decadal Variability in the Tropical Mean Radiative Energy Budget. *Science, Vol 295:841-844.*